

ON AUTOMATIC METRIC RADIO MAP GENERATION FOR THE PURPOSE OF WIFI NAVIGATION

Submitted: 15th June 2017; accepted 17th October 2017

Piotr Bigaj, Jakub Bartoszek

DOI: 10.14313/JAMRIS_3-2017/30

Abstract:

We present a novel method of fast and reliable data gathering for the purpose of location services based on radio signal strength services such as WiFi location/navigation. Our method combines the acquisition of location and mapping based on computer vision methods with WiFi signal strength stochastic data gathering. The output of the method is threefold: 3D metric space model, 2D floor plan map and metric map of stochastic radio signal strength. The binding of location data with radio data is done completely automatically, without any human intervention. The advantage of our solution lies also in a significant speed-up and density increase of Radio Map generation which opens new markets for WiFi navigation services. We have proved that presented solution produces a map allowing location in office space of accuracy 1.06 m.

Keywords: *indoor positioning, radio map, mobile devices, WiFi fingerprint localization, path planning*

1. Introduction

In classic approach WiFi indoor location is based on fingerprinting [1, 4–10]. Fingerprinting is a way of representing a Radio Map as a set of metric positions combined with WiFi BSSID's (Basic Service Set Identifier) and their RSSI (Received Signal Strength Indication). Such map is then used as a reference: a user willing to localize its terminal compares the radio-strength distance of its current location with the locations on the map and choosing the one with the closest distance. The most important aspect is a way of calculating the radio-strength distance between user's location and locations from a map.

Apart from location estimate methods there is a crucial aspect influencing the quality of location services: namely a Radio Map, the quality of which determines the accuracy of location itself. Therefore a construction of the Radio Map is fundamental for further location.

2. Problem Statement

In the research described within the scope of this paper the goal is twofold.

The first is to propose a method that minimizes the time of gathering the large amount data for wireless Radio Map. For this purpose we support automa-

tic receive signal strength indication measurements with SLAM (Simultaneous Localization and Mapping) approach.

The second goal is to propose novel method of location estimation based on previously prepared Radio Map. In this goal we want to minimize location errors represented by circular error probability measure. This is achieved by introducing divergences and metrics calculations for Radio Maps stored in a form of a set of probability distribution of RSSI signal.

3. Organization of the Paper

The remaining part of article is organized as follows: Paragraph 4: describes state-of-the-art for Radio Map generation method and their drawbacks. Paragraph 5: describes the motivation to create an automatic method for creating WiFi stochastic metric Radio Map. Paragraph 6: describes a high-level approach by presenting and distinguishing between two pipelines of calculations: SLAM and Wireless pipeline. Paragraph 8: Describes how metric locations are gathered and how a floor plan is calculated based on that measurement. Paragraph 9: Details how wireless measurements are taken and stored as well as it describes a list of methods to calculate the location data. A description of single-value and f-divergences are given. Paragraph 10: Explains results of experiments done for validation of proposed approach and to assess the quality of proposed solution. Paragraph 11 and 12: lines up conclusions of the work and presents future plans.

4. Current Radio Map Generation Methods

In current approaches [1, 2] a Radio Map is generated in a following sequence: a human user plans a path to walk through locations in which he will gather the RSSI. He stops on every planned point, measures the radio signal strength and moves to next point where the procedure of measurement repeats. While this approach is obvious and natural it also has serious limitations. (1) The user needs to position himself in the exact location as planned, otherwise the location measurement error will also include mismatch of the Radio Map. (2) The user needs an a priori known map (or plan of the building) to plan his path. (3) The output of such procedure is a list of locations with assigned radio signal strength information and it has no automatic correspondence with a map. (4) The location on such Radio Map has to be manually annotated with metric data, which excludes the use of such Radio Map from a systematic approach for POI placement.

Other approach of Radio Map generation involves collection of data samples gathered by service user [3, 11–12]. This approach, despite the many benefits and advantages over the classic methods of collection of data, also requires the preparation of an initial version of the map. Furthermore, in a dynamically changing environment, it is necessary to carry on, with a certain time interval, additional measurements for Radio Map verification.

5. The Motivation

There were a variety of motivation aspects for conducting a research on WiFi surveying. Apart from drawbacks mentioned in previous section the primary motivation to conduct this research was the lack of an automatic and fast method for generating metric Radio Maps. Such automation is especially important when wireless infrastructure changes over time or when an infrastructure needs a rapid setup for limited amount of time e.g. trade fair.

In addition new research [13] on WiFi navigation, points out that stochastic measure of radio signals provides quantitatively and qualitatively better results than classic fingerprinting. This can be explained by a fact that RSSI varies a lot for particular AP in one location over time. This is shown in Fig. 1 – as the number of RSSI samples from AP increases (Fig. 1a) the distribution of RSSI changes significantly. In Fig. 1b samples from corridor-like scenario are shown with their distribution. Both data charts proves that compressing such distribution into one num-

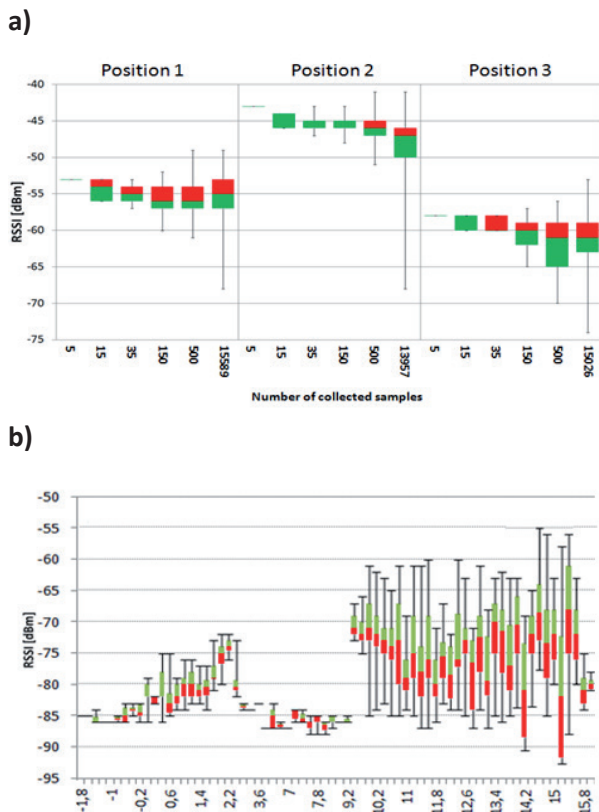


Fig. 1. a) A distribution of RSSI signal for one AP at different locations when number of RSSI sample is varying b) distribution of RSSI in space for corridor-like scenario (user goes through corridor [just x-position is changed] and simultaneously samples RSSI for particular AP)

ber causes loss of information and brings initial error source to location estimation.

Stochastic data gathering is much simplified having an access to metric layer on the Radio Map. Another advantage of new method is that the spatial density of fingerprints is the most important impacting factor for WiFi location performance [3].

The last motivation was to provide a method that could be implemented on existing infrastructure (like scrubber driers in shopping malls) for creating and updating the Radio Map.

Summarizing due to the (1) low speed of Radio Map generation in current approaches, (2) the need of metric, stochastic information in the Radio Map as well as (3) the low Radio Map density a new automatic way of metric Radio Map creation is highly desired for effective WiFi location services.

6. The Overview of New Approach

The proposed approach for Radio Map data gathering is to combine Simultaneous Localization and Mapping (SLAM) concept with WiFi data gathering (Fig. 2). The data are collected by RGB-D camera (SLAM pipeline) and WiFi network card (Wireless pipeline). SLAM pipeline aims in creating a metric 3D point cloud based on which a Metric Map is created. Wireless pipeline collects the RSSIs of APs visible at particular point. Therefore there are two layers of output data: Metric Map layer and Wireless Map i.e. RSSI layer. Both layers are combined to produce a dense metric Radio Map for further location purposes. Whole process is depicted in Fig. 2.

SLAM pipeline aims at determining the current location of the apparatus. Together with SLAM pipeline a wireless data is gathered as the apparatus is moving. The wireless data contains information of BSSIDs and their RSSIs. The output is gathered in a form of histogram for particular BSSID and its RSSIs in particular location. Such approach is motivated by a fact of non-Gaussianity of the RSSI distribution and is intended to provide as much valuable data for further location al-

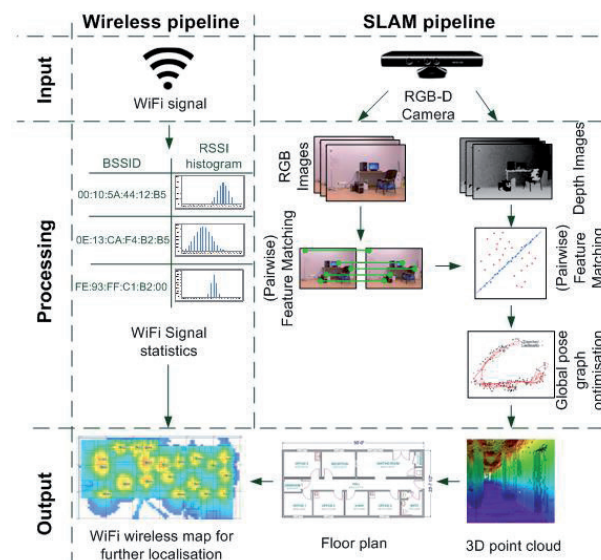


Fig. 2. The procedure of Wi-Fi metric Radio Map data gathering in two pipelines: Wireless and SLAM

gorithm as possible (Fig. 1). This way a simple metrics as well as kernelized probabilistic locations approach can work on same Radio Map. The position of the apparatus calculated in SLAM pipeline allows updating histogram in particular location.

One of advantages of using probabilistic approach is that it significantly reduces the influence of various inferences of radio signal that result in lowering the quality of location process. This means that the immunity of presented system is higher of those based on classic RSSI calculations. These influences are reduced by taking multiple samples of RSSI for each AP in particular location and build a probability distribution of these samples. In this method we assign a probability to particular value of RSSI i.e. we estimate what is the probability of this particular RSSI to be receive in that location. The influence of RSSI changes due to various inferences such as people passing by are therefore reduced since such distortion will be projected only in a part of signal strength distribution. This stochastic approach has also an impact on noise immunity.

7. Radio Map Construction

Metric Radio Map M is a set of points M_i . Each of the point on the WiFi metric Radio Map combines two values:

$$M_i = (M_{i,loc}, P_i) \quad (1)$$

$M_{i,loc}$ – metric location. This location is calculated by SLAM pipeline (Fig. 2). $M_i = (x_p, y_p)$.

P_i – RSSI probability density function in location $M_{i,loc}$ calculated by maximum likelihood estimation for samples gathered in location $M_{i,loc}$. This is calculated by Wireless pipeline (Fig. 2) The probability density function is multinomial: it contains information about probability distributions for multiple APs in the location $M_{i,loc}$:

$$P_i = (p_{AP1,i}, p_{AP2,i}, \dots, p_{APn,i}) \quad (2)$$

$p_{AP1,i}$ – RSSI probability density function in location $M_{i,loc}$ for particular AP (AP_i) having particular value of RSSI. This probability density function is calculated by maximum likelihood estimation and therefore it can be considered as a scaled histogram.

8. SLAM Pipeline

SLAM produces a Metric Map consisting on a set of locations in which the apparatus was present ($M_{i,loc}$). Each time the apparatus moves producing new $M_{i,loc}$ new location is added to Radio Map M .

With the apparatus position changes RGB and Depth images are collected and compared with previous ones. The first comparison is done for RGB image for matching visual features. Algorithm used for this purpose is strictly dependent on the platform used for data collection. The user should make a choice between algorithms SIFT / SURF and ORB. The first two proposed algorithms allow for better accuracy, however, require more computing power. The third algorithm, which gives the worst results, is suitable for use on mobile platforms. Below (Fig. 3)

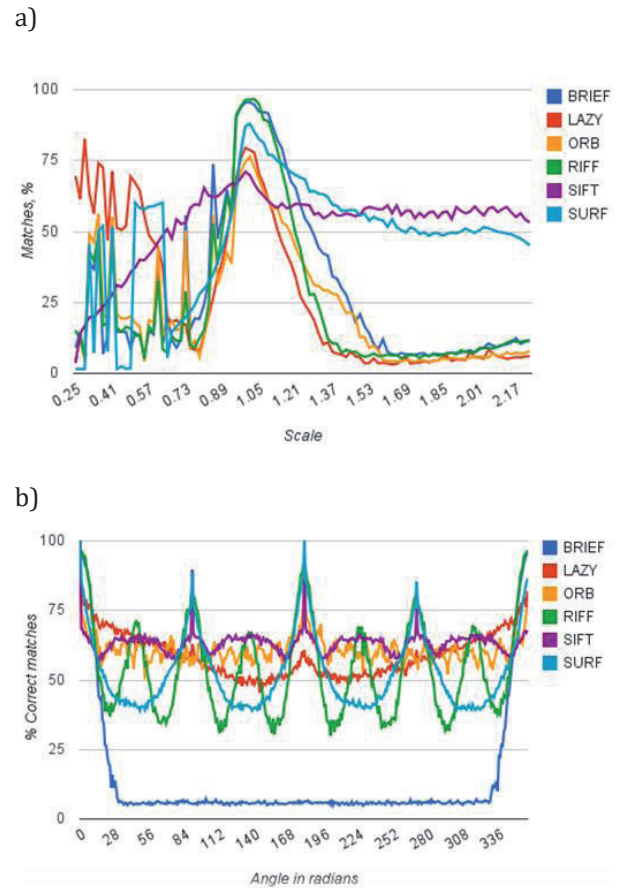


Fig. 3. Comparison of matching algorithms due to: a) changing the distance from the object. b) changing the orientation of the camera, Source: [14]

one can find graphs showing the effect of changing the orientation of the camera and the distance from the captured object to the obtained results. These indicate clearly that in the case of using a mobile platform with less computing power it is necessary to ensure a stable position of the camera, and it's relatively slow movement (slow walk). Moreover, the use of a platform with lower computing power will prevent collection of data in an environment with a low degree of differentiation and with low details (e.g. hallway with white walls).

Second step of method is based on preselecting a pair wise (between two acquisition points) 6D transformation estimation: RANSAC [15] for visual data, Global Iterative Closest Point algorithm for point cloud. This order is result from the need to reduce the amount of calculations required to determine the exact camera shift. At the first the displacement is determined with less accuracy and next based on that the more detailed solution is calculated. In next step a pose graph optimization is run (g2o) on data from matched 3D point cloud. As a result point cloud (coloured by RGB image) is added to metric 3D model. Unfortunately, it is impossible to avoid drift occurring during data collection; therefore it is necessary to close the loop for long straight sections of the route (over 10m) in order to minimize the location error. The last step of proposed method is projecting 3D model (Fig. 4a) on XY surface to produce metric 2D map (Fig. 4b).

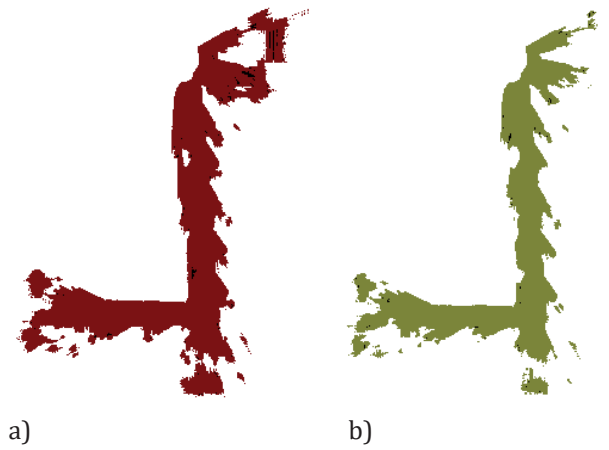


Fig. 4. Partial point cloud visualisation: a) Whole point cloud, b) Detected floor

The density of a map understood as an average distance between consecutive points is therefore dependent of the velocity of measuring device. With our implemented SLAM pipeline we have achieved an average density of 0.10 m in office space for average velocity of movement 1.4 m/s (typical walking speed of human). Feature matching, global pose estimation and 3D point cloud are generated whilst apparatus moves (i.e. all calculations are done online, without uploading it to a cloud). An example of three steps of map creation is shown in figure below (Fig. 5).

Due to a drift in Global Pose estimation it is always better to close the loop while moving to reduce this drift. When the loop is not closed (Fig. 5a) straight segments of movement become curved due to drift. When feature matcher has matched “end” of the loop with the “beginning” (Fig. 5b) global pose graph optimization corrects such drift.

Locations of $M_{i,loc}$ do not have to be known a priori, before the map building process is started. $M_{i,loc}$ are calculated along with SLAM apparatus movement. The only limitation of the sampling locations is that during map building the apparatus needs to visit positions $M_{i,loc}$ in which further location will be performed. This means that the apparatus needs to appear wherever human will need location service. On the other hand if the apparatus appear multiple times in one location or in the proximity of that location the map is updated by adding wireless signal information to that location. This means that deployment and maintenance cost of surveying system is negligible, as it needs only the SLAM apparatus.

9. WiFi Pipeline

Our method of wireless data gathering and processing can be described as follows: In order to perform location we need to find the metric position $L = (x_p, y_p)$ in that particular point. To achieve that we sample the distribution Q of RSSI for multiple APs ($Q = (q_{AP,1}, \dots, q_{AP,n})$) is multimodal as P_i in each location $M_{i,loc}$ is). Next we need to compare Q with P_i for each location $M_{i,loc}$. This comparison aims in providing a single number that shows how similar is the distribution of RSSI signals in the location that we currently measure (Q distribution) to each of previously measured distributions (P_i

in $M_{i,loc}$ in the Radio Map M). Based on this comparison we estimate L as L in the position in which Q was taken ($\bar{L} = (\bar{x}_l, \bar{y}_l)$). Therefore the key aspect in location is to calculate a distance between Q and P_i distribution. The comparison between Q and P_i is a comparison of a discrete probability density functions. In order to make such comparison we use and compare different approaches including: comparing single values represented by mean and median values, probability density divergences and density metrics i.e. f-divergences [16–18].

In current approach the number of P_i distributions equalling number for visited locations ($M_{i,loc}$) has an impact on systems performance. This is because the calculation of location estimation demands a comparison of Q and P_i distribution. The number of comparisons depend on number of points in the Radio Map in the linear manner and so does the time complexity of the location ($O(n)$). In practice we have calculated the location of a terminal on the map of order of 10^3 points (30×25 m) in 5 ms on a typical desktop computer.

In following chapters three groups of methods will be discussed.

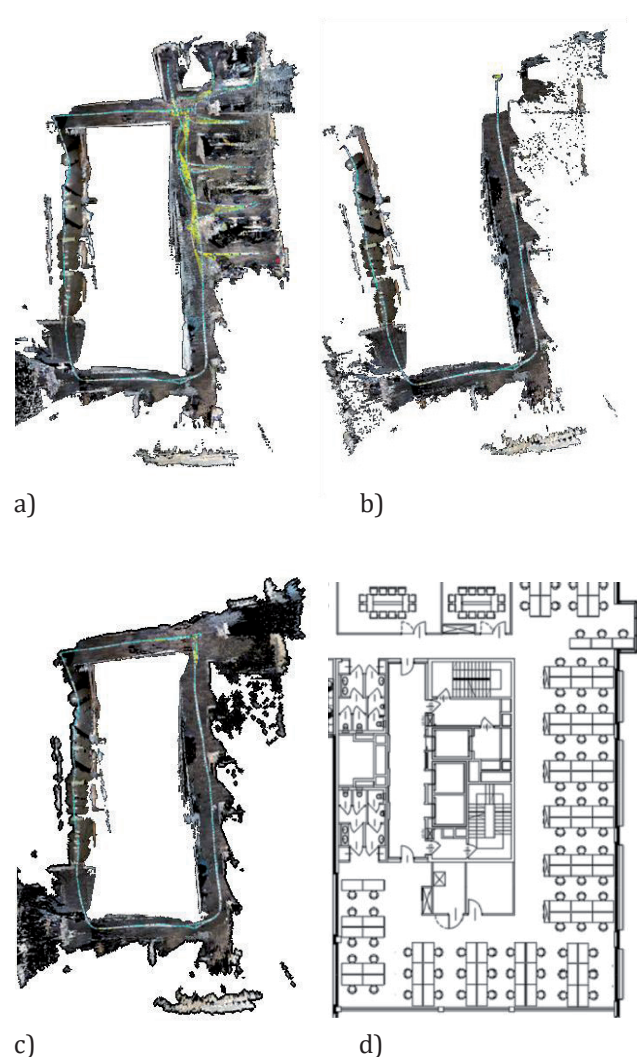


Fig. 5. Consecutive steps of metric map generation by our algorithm at office space (30 x 25m). a) The loop is not closed and in further part of path a drift starts to play significant role b) the loop is closed and drift is minimised c) whole floor model, d) original floor plan

9.1. Single Value Based Calculations

For single value based calculations we compress the distributions Q and P_i to single value of mean or median of these. The distance between Q and P_i is calculated as a distance between vectors of means or medians of Q and P_i . This is done in following steps:

Calculate means or medians for distributions Q and P_i : \bar{Q} and \bar{P}_i .

Calculate distance between vectors \bar{Q} and \bar{P}_i :

$$d(Q, P_i) = \begin{bmatrix} d_1 \\ \dots \\ d_i \end{bmatrix} \quad (3)$$

$$d_j = \begin{cases} |\mu_{p_{AP,j}} - \mu_{q_{AP,j}}| & \text{for AP in } Q \text{ and } P_i \\ |\mu_{p_{AP,j}} - S| & \text{for AP in } P_i \text{ and not in } Q \\ |\mu_{q_{AP,j}} - S| & \text{for AP in } Q \text{ and not in } P_i \end{cases} \quad (4)$$

S – a sensitivity of a receiver and $\mu_{p_{AP,i}}$ is a mean value of RSSI in distribution $p_{AP,i}$. For our case $S = -120$ (120 dBm is a sensitivity level of our wireless card).

Calculate the norm of a vector:

$$D(Q, P_i) = \sqrt{\sum_i d_i} \quad (5)$$

9.2. Divergence-Based Calculations

In probability theory a divergence is a function that measures the difference between two probability distributions. We assume local independence of probability distribution for different AP. Thanks to this assumption the total divergence of and is a sum of divergences between distributions of the corresponding AP's RSSI:

$$D(Q||P_i) = D_{diff}(Q||P_i) + D_{comm}(Q||P_i) \quad (6)$$

$$D_{diff}(Q||P_i) = \sum_i D(q_{AP,i}||p_\alpha) \quad (7)$$

$$D_{comm}(Q||P_i) = \sum_i D(q_{AP,i}||p_{AP,i}) \quad (8)$$

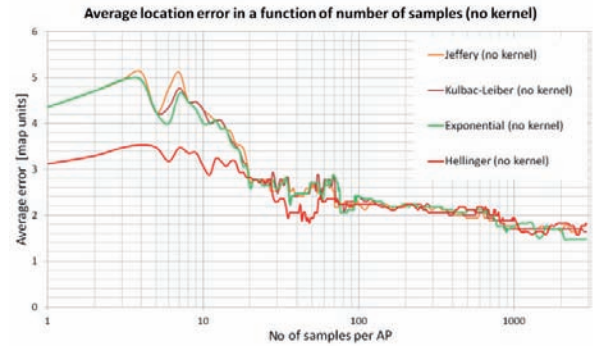
$D_{diff}(Q||P_i)$ – divergence for AP's that are present in distribution Q (location L) i.e. when $p_{AP,1} = \mathbf{0}$,

$D_{comm}(Q||P_i)$ – divergence for AP common in and Q , p_α – is a small constant. Its function is explained below.

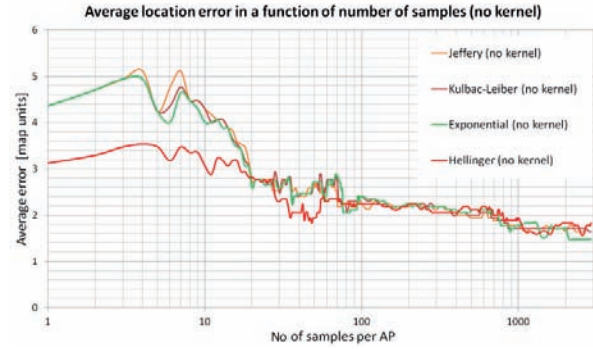
Note that $D(Q||P_i)$ is non symmetric i.e. in general $D(Q||P_i) \neq D(P_i||Q)$. Therefore to symmetrise a symmetric divergence is introduced:

$$D(Q, P_i) = D(Q||P_i) + D(P_i||Q) \quad (9)$$

In our approach we use four different divergences: Kullback-Leiber [19–20], Jeffrey [21–22], Kagan and Exponential. Realisation of (7) and (8) is for these divergences presented below:



a)



b)

Fig. 6 a) Mean location error in function of number of samples gathered for non-kernel divergences (calculated by combining Method 1 of section 9.4 with divergences of (12),(15),(18),(21) and Method 1 of section 9.4 with Hellinger distance of (24)), b) 50-th percentile of location error in a function of number of samples for kernelled method (calculated by combining Method 3 of section 9.4 with divergences of (12), (15), (18), (21) and Method 3 of section 9.4 with Hellinger distance of (24)). The error units are equal to Metric Map density, for this case was 1m

9.2.1. Kullback-Leiber Divergence

$$D_{KL_diff}(q_{AP,i}||p_\alpha) = \sum_x q'_{AP,i}(x) \ln \frac{q'_{AP,i}(x)}{p_\alpha} \quad (10)$$

$$D_{KL_comm}(q_{AP,i}||p_{AP,i}) = \sum_x q'_{AP,i}(x) \ln \frac{q'_{AP,i}(x)}{p_{AP,i}(x)} \quad (11)$$

$$D_{KL}(Q, P_i) = \sum_i (D_{KL_diff}(q_{AP,i}||p_\alpha) + D_{KL_comm}(q_{AP,i}||p_{AP,i})) + \sum_i (D_{KL_diff}(p_{AP,i}||p_\alpha) + D_{KL_comm}(p_{AP,i}||q_{AP,i})) \quad (12)$$

9.2.2. Jeffrey Divergence

$$D_{JEF_diff}(q_{AP,i}||p_\alpha) = \sum_x (q'_{AP,i}(x) - p_\alpha) \ln \frac{q'_{AP,i}(x)}{p_\alpha} \quad (13)$$

9.2.3. Kagan Divergence

$$D_{JEF_comm}(q_{AP,i}||p_{AP,i}) = \sum_x (q'_{AP,i}(x) - p_{AP,i}(x)) \ln \frac{q'_{AP,i}(x)}{p_{AP,i}(x)} \quad (14)$$

$$D_{JEF}(Q, P_i) = \sum_i (D_{JEF_diff}(q_{AP,i}||p_\alpha) + D_{JEF_comm}(q_{AP,i}||p_{AP,i})) + \sum_i (D_{JEF_diff}(p_{AP,i}||p_\alpha) + D_{JEF_comm}(p_{AP,i}||q_{AP,i})) \quad (15)$$

$$D_{KAG_diff}(q_{AP,i}||p_\alpha) = \frac{1}{2} \quad (16)$$

$$D_{KAG_comm}(q_{AP,i}||p_{AP,i}) = \frac{1}{2} \sum_x \frac{(q_{AP,i}(x) - p_{AP,i}(x))^2}{q_{AP,i}(x)} \quad (17)$$

$$D_{KAG}(Q, P_i) = \sum_i (D_{KAG_diff}(q_{AP,i}||p_\alpha) + D_{KAG_comm}(q_{AP,i}||p_{AP,i})) + \sum_i (D_{KAG_diff}(p_{AP,i}||p_\alpha) + D_{KAG_comm}(p_{AP,i}||q_{AP,i})) \quad (18)$$

9.2.4. Exponential Divergence

$$D_{EXP_diff}(q_{AP,i}||p_\alpha) = \sum_x q'_{AP,i}(x) \left(\ln \frac{q'_{AP,i}(x)}{p_\alpha} \right)^2 \quad (19)$$

$$D_{EXP_comm}(q_{AP,i}||p_{AP,i}) = \sum_x q'_{AP,i}(x) \left(\ln \frac{q'_{AP,i}(x)}{p_{AP,i}(x)} \right)^2 \quad (20)$$

$$D_{EXP}(Q, P_i) = \sum_i (D_{EXP_diff}(q_{AP,i}||p_\alpha) + D_{EXP_comm}(q_{AP,i}||p_{AP,i})) + \sum_i (D_{EXP_diff}(p_{AP,i}||p_\alpha) + D_{EXP_comm}(p_{AP,i}||q_{AP,i})) \quad (21)$$

Equations (10), (13), (16) and (19) are specific realisation of a sum (7), whilst (11), (14), (17) and (20) of (8). p_α is a small constant ($\sim 10^8$) used in (10), (13) and (16) to avoid taking logarithm of zero. Because p_α is a Laplace-like smoothing stilling some mass probability from parameter the remaining probability distribution, namely $q_{AP,i}$ becomes $q'_{AP,i}$ in (10), (13) and (16). To do so it needs need to be renormalized:

$$q'_{AP,i} = (1 - c \cdot p_\alpha) q_{AP,i} \quad (22)$$

c – number of AP present in distribution Q and not present in distribution $P_i = (p_{AP,i} = \mathbf{0})$.

Due to a fact that p_α is very small e.g. 10^{-8} the difference between $q_{AP,i}$ and $q'_{AP,i}$ are very small. All divergences used here do not satisfy triangle inequality and therefore are premetric. Symmetrising corresponding divergences of (10) and (11), (13) and (14), (16) and (17), (19) and (20) by applying approach of (9) we end up with symmetric divergences. By applying (9) we end up with (12), (15), (18), (21) respectively for Kullback-Leiber, Jeffrey, Kagan and Exponential divergences.

9.3. Metrics-Based Calculations

The similarity between two probability distributions can also be calculated by Hellinger distance [23–25]. Its discreet form is as follows:

$$D_{HELL}(q_{AP,i}, p_{AP,i}) = 1 - \sum_x \sqrt{q_{AP,i}(x) p_{AP,i}(x)} \quad (23)$$

There is no need to deal with common and different AP in this Hellinger's approach as non-existing AP zeroes particular expressions in the sum. Therefore smoothing is also not needed. The total Hellinger distance between two multimodal RSSI distributions is therefore equal to:

$$D_{HELL}(Q, P_i) = \sum_i \left(1 - \sum_x \sqrt{q_{AP,i}(x) p_{AP,i}(x)} \right) \quad (24)$$

9.4. Regression Methods

Using solutions from (12), (15), (18), (21) or (24) one ends up with a table T of length i_{max} (i_{max} is a number of of data points on the Radio Map M). This table represents estimate of distances¹ of the location where the measurement was taken (Q distribution) to each point M_i on the Radio Map with corresponding P_i distribution.

In order to estimate the position of current measurement $\bar{L} = (\bar{x}_l, \bar{y}_l)$ we can use one of three approaches:

Method 1. Pick P_i for which $T[i]$ has the smallest value i.e. choose the nearest neighbour.

Method 2. Sort T increasingly and sort $M_{i,loc}$ accordingly (so that T_i corresponds with location $M_{i,loc}$). Choose k -nearest neighbours and estimate the output location by regular weighted sum:

$$(\bar{x}_l, \bar{y}_l)^T = \frac{\sum_{i < k} (T_{max} - T_i) \cdot M_{i,loc}^T}{\sum_{i < k} (T_{max} - T_i)} \quad (25)$$

$$T_{max} = \max(T_i) \text{ for } i < k$$

Method 3. Sort T increasingly and sort $M_{i,loc}$ accordingly (so that T_i corresponds with location $M_{i,loc}$). Choose k -nearest neighbours and estimate the output location by kernel regression-based weighted sum:

$$(\bar{x}_l, \bar{y}_l)^T = \frac{\sum_{i < k} k(T_i) M_{i,loc}^T}{\sum_{i < k} k(T_i)} \quad (26)$$

¹ Not in mathematical sense.

$$k_1(T_i) = e^{-\beta T_i} = e^{-\beta D(Q,P_i)} \quad (27)$$

$$k_2(T_i) = e^{-\beta T_i^2} = e^{-\beta D^2(Q,P_i)} \quad (28)$$

B – is only a scaling factor added here not to lose numerical precision in case of large $D(Q, P_i)$. It is different for particular realisation of $D(Q, P_i)$: (12), (15), (18), (21) and (24). The kernel can take two forms: simple (27) or Gaussian kernel (28).

Note that, sums of (25) and (26) are limited to nearest neighbours. For comparison we choose to correspond with positions of: mean (μ), 10-, 20-, 30-, 40-, 50-, 60-, 70-, 80-, 90-percentile, $\mu - \sigma$ and $\mu - 2\sigma$ (μ, σ are mean and standard deviation of T (for (25)) and $k(T)$ (for (26)).

Summarising each method of calculation (there are 7 methods) we use 4 types regression and for 3 of them we have 12 different k values. This gives us 273 variants of methods for quality comparison.

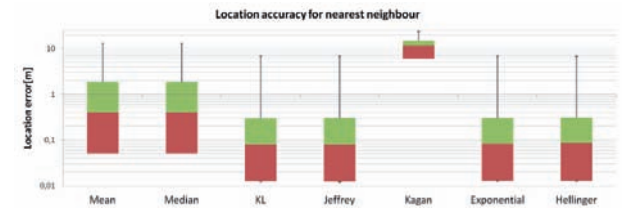
10. Experiments

10.1. Experiment 1: Estimation of Number of Needed Samples

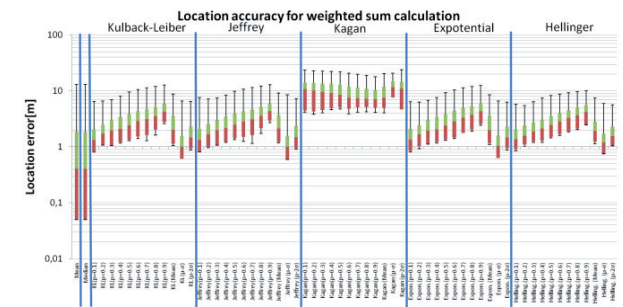
In order to estimate the proper conditions for gathering Radio Map data we have measured what is the desired number of samples per location $M_{i,loc}$ to create RSSI distribution P_i meaningful for the process of location estimation. Such information is needed since samples are gathered by WiFi pipeline while the whole apparatus is moving, therefore the desired number of samples per location limits the velocity of movement while gathering these samples. From one site (D1) one needs to limit number of samples per location $M_{i,loc}$ since the number of samples affects sample gathering time in this particular location and this affects the total time for creation of full Radio Map M . On the other hand we need (D2) many samples to provide P_i distribution that would capture the true distribution of RSSI signals for different AP in location P_i . These demands: (D1) and (D2) are in contradiction and in order to build Radio Map effectively we need to find a good balance between these two.

We have collected a large sample data from 20 locations i.e. a Radio Map consisted of 20 M_i points. Each P_i consisted of distributions of RSSI for particular AP as in (2). For each AP we have collected more than 3000 samples from which p_{AP_i} distribution was build. Data collection for one $M_{i,loc}$ took approximately 360 s giving approximately sampling speed of 150 samples/s. Next we have limited the number of samples per AP in each point $M_{i,loc}$ to 1, 2, 3, ..., 3000 and for such limitation we have build . Next we have extracted points M_i one by one and for each point of the Radio Map M_i we have estimated the location on such limited Radio Map $M' = M - \{M_i\}$ and calculated the error of this estimation. The average error is presented in Fig. 6a, whilst the 50th percentile of an error is presented in Fig. 6b. Units of error are not significant in this experiment as it strictly depend on how sparse the locations of $M_{i,loc}$ are – only the dependency type is important here. One may notice that the error of location estimation both for average and 50th percentile starts to

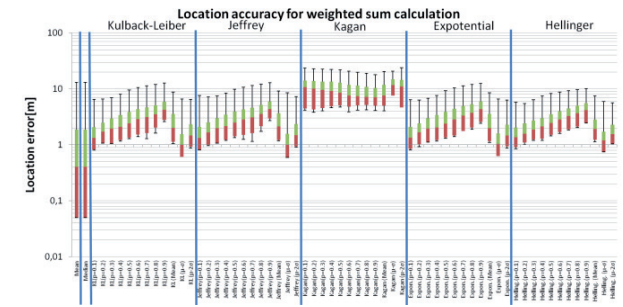
rapidly decrease for Radio Maps of at least 10 samples for AP this decrease is stabilised around Radio Map of 35 samples. On the other hand having a Radio Map of over 3000 samples per AP per location is redundant as the location performance for a Radio Map of over



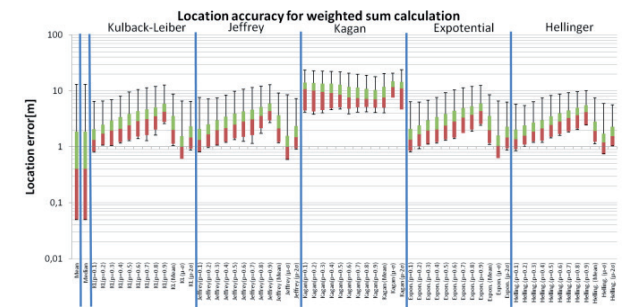
a)



b)



c)



d)

Fig. 7. Location errors for different modes of calculations. Mean and median (first two) based calculations are provided as a baseline: a) nearest neighbour – section 9.4. Method 1, b) Weighted sum calculation – section 7.4. Method 2, c) Kernel based calculation for k_1 kernel – section 7.4. Method 3 d) Gauss kernel based calculation for k_2 kernel – section 7.4. Method 3. All methods (x-axis) are KL-Kullback Leiber, Jeffrey, Kagan and Exponential divergence, Hellinger Distance. k – limitation of length in weighted sum and kernel methods is set to be: $p=0.1...0.9$ – percentile 0.1...0.9 of distribution, μ – mean value of distribution, $\mu - \sigma$ – mean minus standard deviation, $\mu - 2\sigma$ – mean minus two standard deviations

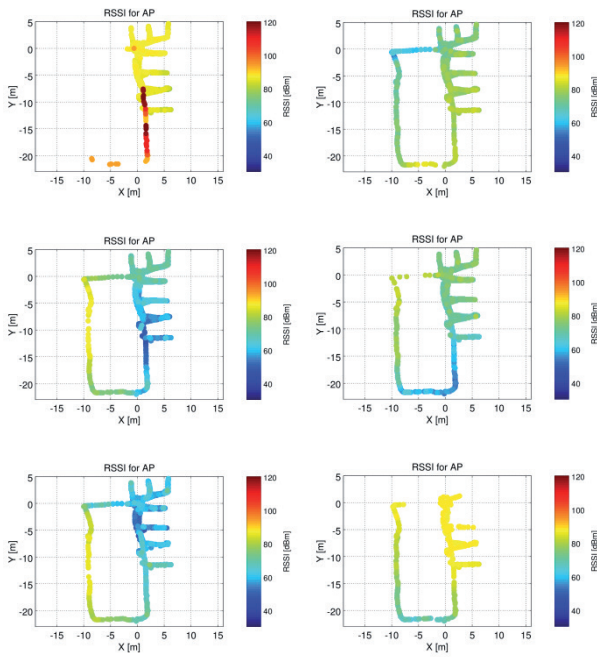


Fig. 8. RSSI signal from 6 different AP in the Radio Map M

1000 RSSI samples per AP is almost constant for such Radio Maps. Summarising: a time of 1 s of sampling gives on average 150 samples per AP. In the result we estimate, that 35 samples for AP is enough for efficient location using proposed methods. A time of 0.2(3) s of sampling in one location is therefore enough to produce Radio Map point M_i with effective calculation for methods described in chapter 7 Average number of APs for this scenario was 24 and points where gathered with density of 1 m. Since the process of RSSI sampling is continues in sense that the apparatus is in movement while measuring WiFi signal we have to assign some distribution P_i gathered on the movement to one location $M_{i,loc}$. Since the location accuracy of presented method i.e. the primary location accuracy of $M_{i,loc}$ calculated by SLAM pipeline is several centimetres this location estimation has to be rounded to higher (worse accuracy) number e.g. 50 cm. This means that all RSSI samples in the range of 50 cm from $M'_{i,loc}$ will be bonded to that location ($M'_{i,loc}$). Assuming a linear movement (constant velocity), sampling achieved speed of 150 samples/s, calculated 35 samples the and a map of a grid of 50 cm we achieve maximum velocity of apparatus of 2.14 m/s. The preferred walking velocity is 1.4 m/s, therefore our solution allows to exceed this velocity. When moving with the preferred walking velocity we can achieve over 54 samples per AP. On the other hand preferred walking velocity allows gathering samples of minimum quantity (35 samples per AP) with the grid of 30 cm. Summarizing the proposed method allows it to be used by both: walking human and a robot, because WiFi sampling time is low enough to gather the representative set of RSSI samples for further distance calculations.

10.2. Experiment 2: Office Location – Comparison of the Points of Radio Map

During this experiment a Radio Map M of an office building was taken by SLAM method described ear-

lier. In this office space of approximately $30\text{ m} \times 25\text{ m}$ a Radio Map M was created and set of locations (L_i, Q_i) was taken in the same location. Number of Radio Map points is $i_{max} = 1172$. The procedure of estimating location error was similar to the one described in section 10.1: for each i -th point in the Radio Map set this point as location $L = M_{i,loc}$, $Q = P_i$, and remove from the Radio Map $M: = M - \{M_i\}$. For each of point we have calculated location errors for each method: single value (section 9.1), divergences (section 9.2) and metrics (section 9.3). For all calculations we have used non-regression and regression methods according to section 9.4. Location errors for these combinations are shown in figure below (Fig. 7).

Worst accuracy is achieved by Kagan Divergence for all modes of calculation (NN, weighted sum and kernel).

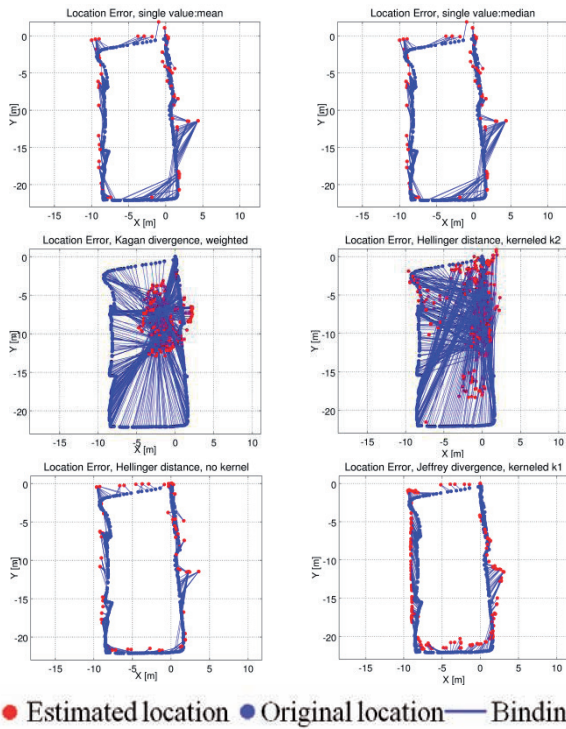
In this scenario we have achieved best performance for non-kernelled NN methods. 50% of locations estimated by Nearest Neighbour Jeffrey divergence are inside a circle of radius of 0.079 m. For Exponential divergence NN 95% of locations provided by estimate are in 1.06 m of radius. Nearest Neighbour get the location of a point with smallest divergence/distance value. Therefore such good results for Nearest Neighbours can be explained by a fact that Radio Map is taken by SLAM with very high density of $M_{i,loc}$. In this Radio Map locations are distanced in average 0.059 m so that the Radio Map is very dense. Average number of APs was 35.

10.3. Experiment 3: Office Location – Location Accuracy

In this experiment we have created a Radio Map of environment M . A view of RSSI levels for several AP is presented in Fig. 8.

In this experiment we have gathered the Radio Map M of the office space and a set of locations L of the same office space. M and L were gathered using our method for Radio Map gathering, therefore when calculating $\bar{L} = (\bar{x}_i, \bar{y}_i)$ we were able to calculate an error $E_{M,L}$ of positioning by comparing it with L measured by SLAM. $E_{M,L}$ has two components: SLAM error component and WiFi location component. SLAM error component comes from the fact, that Metric Map produced by SLAM is not ideal: estimating location of each point of the Radio Map bears an error E_{SLAM} (E_{SLAM} is estimated in office space in our method approximately 0.3 m). The total $E_{M,L}$ for selected methods is shown in graphical form Fig. 9, whilst numeric values can be found in Tab. 2.

In the best case (Hellinger distance with no-kernels) we have achieved a location accuracy of 1.06 m for 0.5 percentile of measurements (CEP=50) whilst almost all measurements (95th percentile) are below 3 m of error (see results and comparison with other methods in Fig. 10). The subsequent locations estimated by algorithm based on non-kernelized Hellinger distance well mirrors the original path as can be seen by trajectory and bindings presented in Fig. 9e. Please note that trajectory estimation is not supported by any other Bayesian-like filter, but rather is a raw output from location engine. A support of such fil-



● Estimated location ● Original location — Binding

Fig. 9. Location errors for office-like scenario for different methods of location estimation. Bindings lines connect the location L with calculated estimate \bar{L} . a) and b) are given as a baseline, c) and d) are worst results, e) and f) are best results. a) Single value calculation for mean value (section 9.1), b) Single value calculation for median value (section 9.1), c) Location estimated by Kagan divergence weighted sum for $k=40$ th percentile of T ((18) with section 9.4, Method 2), d) Location estimated by Hellinger distance kernelled for $k=90$ th percentile of T ((24) with section 9.4, Method 3, kernel k_2), e) Location estimated by Hellinger distance no kernelled ((24) with section 9.4, Method 1), f) Location estimated by Jeffrey divergence kernelled with $k= \mu(T)$ ((15) with section 9.4, Method 3, kernel k_1) Refer to Tab. 2 for numerical data

ter would only increase quantitatively the quality of our results.

In addition to presented test a cumulative distribution of location error was measured for this scenario. Fig. 10 refer to six selected examples of location estimation method (see Tab. 2 and Fig. 9). We achieve 80th percentile of below 2 m.

11. Related Work

Indoor navigation problem has recently been investigated with different contexts and principals of operation [26–30]. Despite large research attention, commercial indoor navigation solutions are still not very popular. Literature review state two reasons to support this fact [31–33], namely they are (1) Need of higher accuracy in comparison to outdoor solutions and (2) High cost of RF fingerprinting. Accuracy of the order that GPS provides for indoor scenarios: in a mall or in a train station can in fact mislead the user, as the location estimation error can cause pointing to a different store or platform. Unfortunately this problem is even more visible when we compare positioning accuracy in all three dimensions. In real conditions when device has been moved between of-

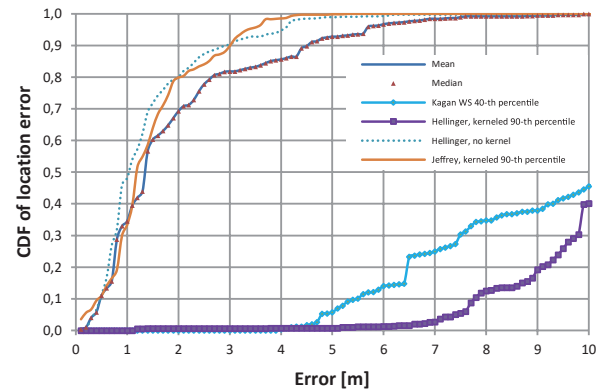


Fig. 10. Cumulative error probability for chosen methods

fice floors most of available systems are not reliable in determining the right position. User has to move for a while to get the precise location.

High cost of RF fingerprinting and a necessity of repeating fingerprinting for building up-to-date map is another drawback of RF-based indoor location method. Even through RF fingerprints (signatures) are widely available in indoor environments they vary over time. Moreover the signatures are sensitive to high usage of APs, number of connected devices and even to human presence. A part from this in public places the infrastructure and is changing over time e.g. every shop is changing decoration every season.

In the environments where global positioning system is not available, the most popular solutions are these based on training sets of signatures annotated with the ground truth (fingerprinting) [34–36]. They provide accurate results and in most cases they do not need any additional hardware. Latest proposed solution try to utilize already available wireless signals, mostly in form of received signal strength indicator – RSSI [32–37]. In this group of solutions that can be called a baseline, location accuracy is in a high correlation with fingerprinting density (e.g. PinLoc [38], Radar [34] and Horus [36]). This particular feature makes the fingerprinting process cost ineffective when higher accuracy is needed since the sample gathering process is manual, performed by a human operator. There are many elaborations proposing solutions to this problem, but most of them determine a set of locations that need more fingerprints.

Another group of solutions is based on customised beacons placed in fixed positions that allow further optimisation for indoor localization algorithms. Those beacons make a use of variety of different wireless technologies e.g. RFID [39], Bluetooth [40], FM signal transmitters [41, 42], ultrasounds [43], infrared [44] and VLC [45–48]. Whilst in general they provide higher location accuracy, they demand additional infrastructure with further need of servicing that increases the overall cost of the system.

The third group can be described as infrastructure-less or self-calibrating. In general those methods do not use any a priori known data about environment. In most cases, they do gather all of the used data directly from users. The biggest advantage of this group in comparison to previously mentioned systems is a low cost of deployment. Unfortunately they also provide the lowest accuracy. Recent elaboration intro-

ducing EZ [49] proposes a solution based on idea that location based on WiFi APs and RSSI can be improved by checking it with GPS on signal availability. Median accuracy achieved after such modification is between 2 and 7 m. Different approach to infrastructure-less localisation was introduced in [50, 51] where authors proposed a solution based on internal inertial sensors of mobile devices. Dead-reckoning accuracy in most cases suffers from the accumulated error from accelerometer [53]. To improve its performance modifications similar to [49] were tested [53, 54]. Slightly better performance was achieved by UnLoc [31] and other solutions [30, 55] that combine dead-reckoning approach with signature detection.

12. Conclusion

The goal of this research was threefold: First we wanted to speed-up a process of wireless Radio Map data gathering, reducing one of the main drawbacks of fingerprint-based location methods. Our approach of Radio Map data gathering uses capabilities of SLAM to correctly bind a metric location with WiFi radio strength signal. Thanks to such approach the output Radio Map is gathered automatically with correct binding of metric position and WiFi signal strength statistics. Our method outperforms classic approach of Radio Map data collection with respect to Radio Map density, location error, time needed for Radio Map creation and automatic generation of a ready-to-use Radio Map. Since the WiFi Radio Map is generated as the apparatus moves we have received up to 10 times faster Radio Map generation comparing with classic methods. This yields the usage of our approach in highly dynamic environments like trade fairs, shopping centres etc.

The second goal was to propose novel method of location estimation based on previously prepared Radio Map. For the purpose of location estimation we proposed to use f-divergences (Kulback-Leiber, Jeffrey, Kagan and exponential divergence) and Hellinger distance together with nearest neighbour approach and 2 types of regression. It is legitimate to state that our method of Radio Map data gathering outperforms the classic, human assisted wireless Radio Map generation approach in sense of Radio Map creation speed and time and Radio Map density. Our method produces a Radio Map of density of 0.05 m (in comparison with approx. 2.5 m for classic approach) density with average speed of sample gathering of 0.2 s (approx. 2 s for classic approach). This result is a significant progress in WiFi surveying.

Thanks to using multiple samples of RSSI the location process is immune to noise and abrupt RSSI changes caused by various inferences e.g. people passing by during sampling. This makes the process of building a Radio Map and then location estimation possible in non-laboratory conditions. This can be explained by the fact that we use stochastic methods for calculations thanks to which we assign small probability to events that occurs rarely in particular location dismissing their influence on further location estimation. The susceptibility to such events is a common issue for signal-strength based localization.

Experimental results of location estimation error show also that proposed solution of using stochastic measures is superior to current solutions presented in the literature [56, 57] even though we do not use any additional source of information than WiFi RSSI. Our solution does not use any additional information to WiFi signal and still it outperforms new systems presented in literature. In space-like scenario we have achieved a result of circular error probability of 1,06 m for office and still show very good performance in 80th percentile of cumulative error probability equal to 2 m for office-like scenario.

13. Future Work

For future work we plan to introduce a method of estimating the quality of Radio Map built automatically so that our solution may be supplemented by autonomous robotic mobile platform that would gather the Radio Map automatically without human intervention.

ACKNOWLEDGEMENTS

The project has been financed by the National Science Center under Decision No. DEC-2012/07/N/ST7/03470.

AUTHORS

Piotr Bigaj* – assistant professor at Industrial Research Institute for Automation and Measurements PIAP, Warsaw, Poland. E-mail: pbigaj@gmail.com

Jakub Bartoszek – research specialist at Industrial Research Institute for Automation and Measurements PIAP, Warsaw, Poland.

*Corresponding author

REFERENCES

- [1] M. Honary, L. Mihaylova, C. Xydeas, „Practical Classification Methods for Indoor Positioning”, *Open Transportation Journal*, no. 6, 2012, 31–38.
- [2] J. Biswas, M. Veloso, „WiFi localization, navigation for autonomous indoor mobile robots”. In: *2010 IEEE International Conference on Robotics, Automation – ICRA*, 4379–4384. DOI: 10.1109/ROBOT.2010.5509842.
- [3] P. Kemppi *et al.*, „Hybrid positioning system combining angle-based localization, pedestrian dead reckoning, map filtering”. In: *IPIN– 2010 International Conference on Indoor Positioning, Indoor Navigation*, 2010. DOI: 10.1109/IPIN.2010.5646682.
- [4] P. Mirowski *et al.*, „KL-Divergence Kernel Regression for Non-Gaussian Fingerprint Based Localization”. In: *International Conference on Indoor Positioning, Indoor Navigation*, Guimaraes, Portugal, 2011.
- [5] N. Le Dortz *et al.*, „WiFi fingerprint indoor positioning system using probability distribution comparison”. In: *2012 IEEE International Conference on Acoustics, Speech, Signal*

- Processing – ICASSP, 2301–2304. DOI: 10.1109/ICASSP.2012.6288374.
- [6] D. R. Brown, D. B. Dunn, „Classification schemes of positioning technologies for indoor navigation”. In: *2011 Proceedings of IEEE Southeastcon*, 125–130. DOI: 10.1109/SECON.2011.5752919.
- [7] V. Moghtadaiee, A. G. Dempster, „WiFi fingerprinting signal strength error modeling for short distances”. In: *International Conference on Indoor Positioning, Indoor Navigation*, 1–6, 2012, Sydney, Australia. DOI: 10.1109/IPIN.2012.6418852.
- [8] C. Beder *et al.*, „Predicting the expected accuracy for finger-printing based WiFi localisation systems”. In: *International Conference on Indoor Positioning, Indoor Navigation*, 1–6, 2011, Guimaraes, Portugal. DOI: 10.1109/IPIN.2011.6071939.
- [9] Z. Hengzhou *et al.*, „Indoor Location Service Based on Finger-printing, Distance Relative Attenuation Model”. In: *2014 Sixth International Conference on Measuring Technology, Mechatronics Automation ICMTMA*, 341–344. DOI: 10.1109/ICMTMA.2014.84.
- [10] C. Beder, M. Klepal, „Fingerprinting based localisation revisited: A rigorous approach for comparing RSSI measurements coping with missed access points, differing antenna attenuations”. In: *International Conference on Indoor Positioning, Indoor Navigation*, Sydney, Australia, 1–7, 2012. DOI: 10.1109/IPIN.2012.6418940.
- [11] J. Ledlie, „Mole: A scalable, user-generated WiFi positioning engine”. In: *International Conference on Indoor Positioning, Indoor Navigation*, 1–10, 2011, Guimaraes, Portugal. DOI: 10.1109/IPIN.2011.6071942.
- [12] P. Bolliger, „Redpin –adaptive, zero-configuration indoor localization through user collaboration”. In: *Proceedings of the first ACM international workshop on Mobile entity localization and tracking in GPS-less environments – MELT’08*, 2008, 55–60. DOI: 10.1145/1410012.1410025.
- [13] P. Mirowski *et al.*, „Probability kernel regression for WiFi localisation”, *Journal of Location Based Services*, vol. 6, 2012, 81–100. DOI: 17489725.2012.694723.
- [14] E. Khvedchenya, *Feature descriptor comparison report*. <http://computer-vision-talks.com/articles/2011-08-19-feature-descriptor-comparison-report/>, 2011. Available on 07.08.2014
- [15] M. A. Fischler, „Random sample consensus: a paradigm for model fitting with applications to image analysis, automated cartography. *Communications of the ACM*, vol. 24, no. 6, 1981, 381–395. DOI: 10.1145/358669.358692.
- [16] H. V. Poor, „Fine quantization in signal detection, estimation”, *IEEE Transactions on Information Theory*, vol. 34, no. 5, 1988, 960–972. DOI: 10.1109/18.21219.
- [17] F. Liese, I. Vajda, „On Divergences, Informations in Statistics”, *IEEE Transactions on Information Theory*, vol. 52, no. 10, 2006, 4394–4412. DOI: 10.1109/TIT.2006.881731.
- [18] M. C. Pardo, I. Vajda, „On asymptotic properties of information-theoretic divergences”, *IEEE Transactions on Information Theory*, vol. 49, no. 7, 2003, 1860–1867.
- [19] D. L. Donoho, X. Huo, „Large-sample modulation classification using Hellinger representation”. In: *First IEEE Signal Processing Workshop on Signal Processing Advances in Wireless Communications*, 1997, 133–136.
- [20] J. R. Hershey, „Approximating the Kullback Leibler Divergence Between Gaussian Mixture Models”. In: *IEEE International Conference on Acoustics, Speech, Signal Processing – ICASSP 2007*, vol. 4, 2007, 317–320. DOI: 10.1109/ICASSP.2007.366913.
- [21] C. Liu, H-Y. Shum, „Kullback-Leibler boosting”. In: *Proceedings of 2003 IEEE Computer Society Conference on Computer Vision, Pattern Recognition*, vol. 1, 2003, 587–594.
- [22] V. N. Murali, „Autonomous navigation, mapping using monocular low-resolution grayscale vision”. In: *IEEE Computer Society Conference on Computer Vision and Pattern Recognition Workshop*, 2008. DOI: CVPRW.2008.4563136.
- [23] J. Svihlik, „Model Parameters Estimation Using Jeffrey Divergence”. In: *17th International Conference Radioelektronika*, 2007. DOI: 10.1109/RADIOELEK.2007.371654.
- [24] F. Topsoe, „Some inequalities for information divergence, related measures of discrimination”, *IEEE Transactions on Information Theory*, vol. 46, no. 4, 2000, 1602–1609. DOI: 10.1109/18.850703.
- [25] A. Ferrante, „Hellinger Versus Kullback–Leibler Multivariable Spectrum Approximation”, *IEEE Transactions on Automatic Control*, vol. 53, no. 4, 2008, 954–967. DOI: 10.1109/TAC.2008.920238.
- [26] Z. Yang *et al.*, „Mobility Increases Localizability: A Survey on Wireless Indoor Localization using Inertial Sensors”, *ACM Comput. Surv.*, vol. 47, no. 3, 2015. DOI: 10.1145/2676430.
- [27] I. Constandache, R.R. Choudhury, I. Rhee, „Towards mobile phone localization without wardriving”. In: *2010 Proceedings IEEE INFOCOM*. DOI: 10.1109/INFOCOM.2010.5462058.
- [28] M. Alzantot, M. Youssef, „CrowdInside: automatic construction of indoor floorplans”. In: *Proceedings of the 20th International Conference on Advances in Geographic Information Systems*, 2012. DOI: 10.1145/2424321.2424335.
- [29] S. Ayub *et al.*, „Indoor pedestrian displacement estimation using smartphone inertial sensors”, *International Journal of Innovative Computing, Applications*, vol. 4, no. 1, 2012, 35–42.
- [30] S. Hilsenbeck *et al.*, „Graph-based data fusion of pedometer, WiFi measurements for mobile indoor positioning”. In: *Proceedings of the 2014 ACM International Joint Conference on Pervasive, Ubiquitous Computing*, 2014.
- [31] H. Wang *et al.*, „No need to wardrive: unsupervised indoor localization”. In: *Proceedings of the 10th international conference on Mobile systems, applications, services*, 2012.

- [32] Y. Chen *et al.*, „FM-based indoor localization”. In: *Proceedings of the 10th international conference on Mobile systems, applications, services*, 2012.
- [33] C. Laoudias *et al.*, „The Airplace Indoor Positioning Platform for Android Smartphone”. In: *Proceedings of the 2012 IEEE 13th International Conference on Mobile Data Management*, 2012, 312–315. DOI: 10.1109/MDM.2012.68.
- [34] P. Bahl, V. N. Padmanabhan, „RADAR: An In-Building RF-based User Location, Tracking System”. In: *Proceedings of INFOCOM*, 2000. DOI: 10.1109/INFOCOM.2000.832252.
- [35] A. Haeberlen *et al.*, „Practical robust localization over large-scale 802.11 wireless networks”. In: *Proceedings of the 10th annual international conference on Mobile computing and networking*, 2004. DOI: 10.1145/1023720.1023728.
- [36] M. Youssef, A. Agrawala, „The horus WLAN location determination system”. In: *Proceedings of the 3rd international conference on Mobile systems, applications and services*, 2005. DOI: 10.1145/1067170.1067193.
- [37] A. Varshavsky *et al.*, „Gsm indoor localization”, *Pervasive Mob. Comput.*, vol. 3, no. 6, 2007, 698–720. DOI: 10.1016/j.pmcj.2007.07.004.
- [38] S. Sen, B. Radunovic, R. R. Choudhury, T. Minka, „You are facing the Mona Lisa: spot localization using PHY layer information”. In: *Proceedings of the 10th international conference on Mobile systems, applications, services*, 2012. DOI: 10.1145/2307636.2307654.
- [39] L. M. Ni, Y. Liu, Y. C. Lau, A. P. Patil, „Landmarc: indoor location sensing using active RFID”, *Wireless Networks*, vol. 10, no. 6, 2004, 701–710. DOI: 10.1023/B:WINE.0000044029.06344.dd.
- [40] R. Bruno, F. Delmastro, *Design, analysis of a bluetooth-based indoor localization system*, Series: *Personal Wireless Communications, Lecture Notes in Computer Science*, 2003.
- [41] A. Matic, A. Popleteev, V. Osmani, O. Mayora-Ibarra, „FM radio for indoor localization with spontaneous recalibration”, *Pervasive Mob. Comput.*, vol. 6, no. 6, 2010, 642–656. DOI: 10.1016/j.pmcj.2010.08.005.
- [42] S. Yoon, K. Lee, I. Rhee, „FM-based indoor localization via automatic fingerprint DB construction, matching”. In: *Proceeding of the 11th annual international conference on mobile systems, applications, and services*, 2013. DOI: 10.1145/2462456.2464445.
- [43] N. B. Priyantha, A. Chakraborty, H. Balakrishnan, „The cricket location-support system”. In: *Proceedings of the 6th annual international conference on mobile computing and networking*, 2000. DOI: 10.1145/345910.345917.
- [44] R. Want, A. Hopper, V. Falcão, J. Gibbons, „The active badge location system”, *ACM Trans. Inf. Syst.*, vol. 10, 1992. DOI: 10.1145/128756.128759.
- [45] Z. Yang, Z. Wang, J. Zhang, C. Huang, Q. Zhang, „Wearables Can Afford: Light-weight Indoor Positioning with Visible Light”. In: *Proceedings of the 13th annual international conference on mobile systems, applications, and services*, 2015. DOI: 10.1145/2742647.2742648.
- [46] Y-S Kuo, P. Pannuto, K-J Hsiao, P. Dutta, „Luxapose: indoor positioning with mobile phones, visible light”. In: *Proceedings of the 20th annual international conference on Mobile computing, and networking*, 2014. DOI: 10.1145/2639108.2641747.
- [47] L. Li, P. Hu, C. Peng, G. Shen, F. Zhao, „Epsilon: a visible light based positioning system”. In: *Proceedings of the 11th USENIX Conference on Networked Systems Design, Implementation*, 2014.
- [48] G. B. Prince, T. D. Little, „A two phase hybrid RSS/AoA algorithm for indoor device localization using visible light”. In: *12th IEEE Global Communication Conference*, 2012. DOI: 10.1109/GLOCOM.2012.6503631.
- [49] K. Chintalapudi, A. Iyer, V. Padmanabhan, „Indoor localization without the pain”. In: *Proceedings of the sixteenth annual international conference on mobile computing, networking*, 2010. DOI: 10.1145/1859995.1860016.
- [50] O. Woodman, R. Harle, „Pedestrian localisation for indoor environments”. In: *Proceedings of the 10th international conference on Ubiquitous computing – UbiComp’08*, 2008. DOI: 10.1145/1409635.1409651.
- [51] F. Li *et al.*, „A reliable, accurate indoor localization method using phone inertial sensors”. In: *Proceedings of the international conference on Ubiquitous computing – UbiComp’12*, 2012. DOI: 10.1145/2370216.2370280.
- [52] A. R. Jimenez, F. Seco, C. Prieto, J. Guevara, „A comparison of pedestrian dead-reckoning algorithms using a low-cost MEMS IMU”. In: *Proceedings of IEEE International Symposium on Intelligent Signal Processing*, 2009. DOI: 10.1109/WISP.2009.5286542.
- [53] M. Youssef *et al.*, „Gac: Energy-efficient hybrid gps-accelerometer-compass gsm localization”. In: *2010 IEEE Global Telecommunications Conference GLOBECOM 2010*. DOI: 10.1109/GLOCOM.2010.5684304.
- [54] J. Liu *et al.*, „Accelerometer assisted robust wireless signal positioning based on a hidden Markov model”. In: *Proceedings of the IEEE/ION Position Location, Navigation Symposium*, 2009. DOI: 10.1109/PLANS.2010.5507251.
- [55] A. W. S. Au *et al.*, „Indoor Tracking, Navigation Using Received Signal Strength, Compressive Sensing on a Mobile Device”, *IEEE Transactions on Mobile Computing*, vol. 12, no. 10, 2013, 2050–2062. DOI: 10.1109/TMC.2012.175.
- [56] L. Hongbo *et al.*, „Accurate WiFi Based Localization for Smartphones Using Peer Assistance”, *IEEE Transactions on Mobile Computing*, vol. 13, no. 10, 2014, 2199– 2214.